Molecular hydrogen in hydrogenated amorphous silicon: NMR evidence

T. Su, S. Chen, and P. C. Taylor
Department of Physics, University of Utah, Salt Lake City, Utah 84112

R. S. Crandall and A. H. Mahan
National Renewable Energy Laboratory, Golden, Colorado, 80401

(Received 7 March 2000)

We measured the concentrations of molecular hydrogen in hydrogenated amorphous silicon (a-Si:H) using a Jeener-Broekaert three-pulse sequence. For samples prepared by both plasma-enhanced chemical vapor deposition (PECVD) and hot wire chemical vapor deposition (HWCVD), the molecular hydrogen concentrations are about one order of magnitude larger than those inferred from spin-lattice-relaxation time (T_1) measurements. There are two distinct environments for hydrogen molecules. In one the molecules are essentially isolated and act as relaxation centers for hydrogen bonded to silicon atoms. In the other, the hydrogen molecules are clustered and do not relax the bonded hydrogen. Samples prepared by HWCVD have a lower transition temperature for freezing of the molecular hydrogen motion than those prepared by PECVD. This behavior is attributed to a more ordered silicon structure in HWCVD samples. The nonexponential behavior of the dipolar relaxation and possible relation with the defects and doping is discussed.

I. INTRODUCTION

Hydrogen plays a crucial role in determining the structural and electronic properties of hydrogenated amorphous silicon (a-Si:H). In typical samples prepared by plasma-enhanced chemical vapor deposition (PECVD), the hydrogen concentration is about 10 to 15 at. %. Most of the hydrogen atoms are bonded to silicon atoms. About 30% of these bonded hydrogen atoms are isolated from one another (dilute); the rest of the bonded hydrogen atoms are clustered. These two different hydrogen environments can be distinguished by proton nuclear magnetic resonance (^{1}H NMR). In ^{1}H NMR the dilute hydrogen produces a narrow line (~ 4 kHz) that is best fitted by a Lorentzian function, while the clustered hydrogen produces a broader line (~ 25 kHz) that is best fitted by a Gaussian function.[1] The presence of a small amount of nonbonded molecular hydrogen in a-Si:H was first proposed by Conradi and Norberg to explain the temperature dependence of the spin-lattice-relaxation time (T_1) of bonded hydrogen.[2] Of the two forms of molecular hydrogen, orthohydrogen (o-H_2) and para hydrogen (p-H_2), only o-H_2 can be detected by ^{1}H NMR, since p-H_2 has a total nuclear spin $I=0$. In the Conradi-Norberg model, H_2 molecules are assumed to be isolated, and the T_1 of o-H_2 is calculated assuming a two-phonon Raman process.[3] The bonded hydrogen is relaxed through these o-H_2 molecules via a rapid spin-diffusion process. Therefore, T_1 of bonded hydrogen is given by

$$T_1(\mathrm{H}) = T_1(\mathrm{H}_2)\frac{n(\mathrm{H})I(I+1)}{\frac{3}{4}n(\mathrm{H}_2)S(S+1)} + T_{1(\mathrm{SD})}, \qquad (1)$$

where I is the nuclear spin of hydrogen and S the nuclear spin of o-H_2, and $n(\mathrm{H})$ and $n(\mathrm{H}_2)$ are the concentrations of bonded hydrogen and H_2, respectively. The fraction $\frac{3}{4}$ accounts for the fraction of molecular hydrogen that exists as o-H_2 at room temperature. $T_{1(\mathrm{SD})}$ is the spin-diffusion-limited, spin-lattice-relaxation time, which is essentially independent of temperature. $T_{1(\mathrm{SD})} \approx 0.16$ s for typical a-Si:H samples prepared by the PECVD technique. This model is supported by the time dependence of the minima of $T_1(\mathrm{H})$ when samples are kept at low temperature.[4] In time, the o-H_2 converts to p-H_2, which reduces the concentration of the o-H_2 molecules and increases the minima of $T_1(\mathrm{H})$. The dependence of $T_1(\mathrm{H})$ on the concentration of o-H_2 agrees well with Eq. (1).[4] From measurements of $T_1(\mathrm{H})$ the concentration of H_2 is about 1% of the total hydrogen in standard samples of a-Si:H made by the PECVD technique. However, this model is based on the assumption that all o-H_2 molecules contribute to spin-lattice relaxation of the bonded hydrogen atoms. Later experimental evidence has shown that this assumption is not correct.[5] It has been recently suggested that molecular hydrogen may play an important role in the metastable effects that are ubiquitous in a-Si:H.[6] Therefore, it is of importance to investigate the presence of hydrogen molecules in a-Si:H in more detail with new NMR techniques. The measurements presented in this paper provide further insight into the local environments for molecular hydrogen in a-Si:H.

As mentioned above, ^{1}H NMR is only sensitive to o-H_2. In addition to its total nuclear spin $I=1$, due to the antisymmetric property of the total wave function of the nuclei, an o-H_2 molecule also has rotational angular momentum $J=1$, with $m_J = 0, \pm 1$. For an isolated o-H_2 molecule, the three rotational states are degenerate, and the wave function is nearly spherical. In solids, the anisotropic crystal field lifts the degeneracy by an energy splitting Δ. For an axially symmetric crystal field, the $m_J=0$ state is the lower-energy state, and the $m_J = \pm 1$ states are at higher energy. For solid hydrogen, Δ is determined by an anisotropic quadrupole-quadrupole interaction between o-H_2 molecules, and $T_c = \Delta/k \sim 1.6$ K, where k is the Boltzmann constant and T_c is a transition temperature corresponding to the energy separation Δ.[7] For $T \gg T_c$, the three rotational states are equally

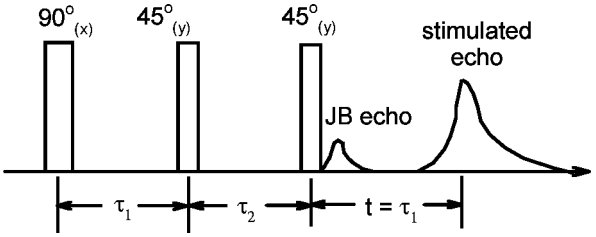

FIG. 1. Schematic diagram of a Jeener-Broekaert sequence. The time intervals between the first and second pulses, and the second and third pulses are τ_1 and τ_2, respectively. Right after the third pulse, a JB echo forms. A stimulated echo forms at $t=\tau_1$ after the third pulse.

populated, and the NMR line shape of o-H_2 is motionally narrowed due to the fast tumbling of the molecules. This motional narrowing results in a line centered at a field determined only by the Zeeman interaction, without any structure. When $T \ll T_c$, the o-H_2 molecules are ''frozen'' into the $m_J=0$ state, and the wave functions are locally ordered with respect to the local crystal field. At these temperatures the resultant NMR line shape of o-H_2 is a powder-averaged Pake doublet. The frequency splitting of the doublet is determined by the dipolar interaction between the two hydrogen atoms in an o-H_2 molecule, which is $\delta\nu=173$ kHz.[8] This Pake doublet provides a unique fingerprint of the existence of o-H_2 at low temperatures.[5]

Unlike solid hydrogen, in which the temperature needed to freeze the o-H_2 is very low, the distorted silicon matrix in a-Si:H produces a large electric-field gradient (EFG), which couples to the electric quadrupole moment of the o-H_2 molecule and provides an additional anisotropic interaction. This interaction can increase T_c to ~ 20 K.[5] Also, below 20 K the signal intensity from o-H_2 is almost independent of temperature, suggesting that most of the hydrogen molecules are frozen below 20 K in a-Si:H.[5]

II. EXPERIMENTAL METHODS

Since the line shape of o-H_2 is very broad, the corresponding time-domain signal decays very quickly. Therefore, any attempt to measure the signal intensity directly from the free-induction-decay (FID), which forms right after a 90° pulse, will suffer severe signal loss due to the finite recovery time of the receiver. In order to obtain accurate measurements of the o-H_2 concentrations, we employed a Jeener-Broekaert three-pulse sequence (JB sequence), shown schematically in Fig. 1. A JB sequence consists of a 90° pulse followed by a pair of 45° pulses that are phase-shifted by 90° with respect to the first pulse.[9] The time separations between the first and the second pulses, and the second and the third pulses are τ_1 and τ_2, respectively. After the second pulse, the spins are converted to the dipolar order, in which the total Zeeman energy vanishes and the total dipolar energy assumes a nonzero value. The third pulse acts as a ''read'' pulse, which converts the dipolar order back to observable Zeeman order. A stimulated echo will form at time $t=\tau_1$ after the third pulse. The amplitude of the stimulated echo can be expressed as[10]

$$f(\tau_1,\tau_2) \propto e^{-2\tau_1/T_2} e^{-\tau_2/T_{1d}}, \tag{2}$$

where T_2 is the spin-spin relaxation time and T_{1d} is the dipolar spin-lattice-relaxation time. Since hydrogen atoms in different environments have different values of T_2 and T_{1d}, we can choose the combination of τ_1 and τ_2 to emphasize a certain component selectively. Also, by extrapolating the dependence of the signal intensity on τ_1 and τ_2 to $\tau_1 \rightarrow 0$ and $\tau_2 \rightarrow 0$, the concentration of o-H_2 can be obtained as a fraction of total hydrogen incorporated. Finally, one can also measure T_1 of o-H_2 by applying a series of 90° pulses (saturating comb) followed by the JB sequence. The dependence of signal intensity on τ, which is the recovery time between the last pulse of the saturating comb and the first pulse of the JB sequence, can be expressed as

$$I(\tau) = I(\infty)(1-e^{-\tau/T_1}), \tag{3}$$

where $I(\infty)$ is the intensity for $\tau \rightarrow \infty$. A plot of $\ln_{10}\{[I(\infty)-I(\tau)]/I(\infty)\}$ against τ will yield T_1 as the slope of the plot.

The experiments were performed on a typical pulsed NMR spectrometer from Tecmag. The spectrometer has two channels for quadrature detection with a 100 ns pulse width resolution. Typical receiver recovery times are ~ 14 μs at 8 K and ~ 5 μs at 300 K. A typical 90° pulse is about 2 μs. A superconducting magnet from Oxford Instruments is used, and the field is set to ~ 2 T, corresponding to a ^{1}H Larmor frequency of ~ 86 MHz. The field inhomogeneity at this frequency is less than 100 Hz over the sample volume. The temperature of the samples is controlled by a dynamic gas exchange cryostat from Oxford Instruments. By using liquid helium as coolant, the sample can be cooled to 1.8 K. During the entire period of the experiments, the temperature can be maintained at a given value with a drift of less than ± 0.5 K.

One sample made by PECVD at the University of Utah and three samples made by hot-wire CVD (HWCVD) at the National Renewable Energy Laboratory were measured at

TABLE I. Growth condition of the PECVD and HWCVD samples.

Sample number	Growth technique	Substrate material	Substrate temperature	Silane concentration	Growth pressure	Hydrogen concentration	Sample thickness
c-10-7-98	PECVD	Al foil	230 °C	100%	200 mTorr	~ 10 at.%	~ 5 μm
THD315[a]	HWCVD	glass	230 °C	100%	10 mTorr	~ 3 at.%	~ 5 μm
THD316[b]	HWCVD	glass	230 °C	100%	10 mTorr	~ 3 at.%	~ 5 μm
H317	HWCVD	Al foil	345 °C	100%	13 mTorr	~ 3 at.%	~ 5 μm

[a]Filament on.
[b]Filament off.

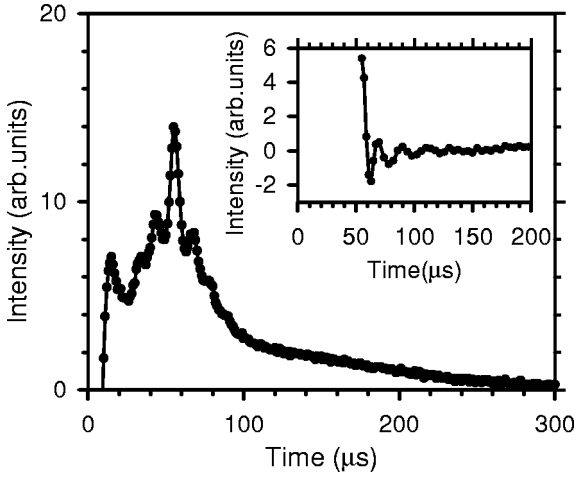

FIG. 2. A typical time-domain signal for the stimulated echo in the PECVD sample. The echo is centered at $t=54$ μs. The inset shows the signal from o-H_2 on an expanded scale. This echo is obtained after subtracting the signal due to bonded hydrogen. The solid lines are aids to the eye.

$T=8$ K. Table I summarizes the growth conditions of these samples. The concentration of o-H_2 were measured by the JB pulse sequence. To infer the fraction of o-H_2 that contributes to the T_1 of bonded hydrogen, the T_1 of bonded hydrogen was measured at 40 K, where the minimum occurs. In addition, the T_1 of o-H_2 was measured at 40 K by applying a saturating comb of pulses followed by a JB pulse sequence.

For typical experimental time scales for cooling down to liquid helium temperature, the slow ortho-para conversion rate preserves the fraction of o-H_2 to p-H_2, which at 300 K is 3:1. Therefore, one can measure the o-H_2 concentration at low temperature and obtain the total molecular hydrogen concentration using the fraction at room temperature.

III. EXPERIMENTAL RESULTS

Figure 2 shows a typical time-domain stimulated echo following the JB pulse sequence for the PECVD sample. The inset shows the signal from o-H_2 after subtracting the signal from that due to bonded hydrogen. The Fourier-transformed spectrum of Fig. 2 is shown in Fig. 3. The Pake doublet that arises from o-H_2 is shown on an expanded scale in the inset in Fig. 3. The linewidths for the broad and narrow central lines are found to be ~ 20 kHz and ~ 4 kHz, respectively. The frequency splitting of the doublet is $\sim 176 \pm 5$ kHz, in good agreement with the theoretical value.[8]

Figure 4 shows the temperature dependence of the Pake doublet for the PECVD sample. As can be seen from Fig. 4, the Pake doublet begins to narrow at $T \sim T_c \approx 20$ K, in agreement with the behavior found in Ref. 5. In contrast, the HWCVD samples exhibit a much lower T_c. Figure 5 shows the comparison of the line shapes from the PECVD and HWCVD samples at $T=8$ K. For the PECVD sample, the Pake doublet is well defined, while for the HWCVD samples, the Pake doublet is narrowed to a structureless central line with a full width at half maximum (FWHM) of ~ 70 kHz (dashed line). Such a narrowing suggests that, even at 8 K, there is still motion of o-H_2 molecules, i.e., the o-H_2 molecules are not completely frozen.

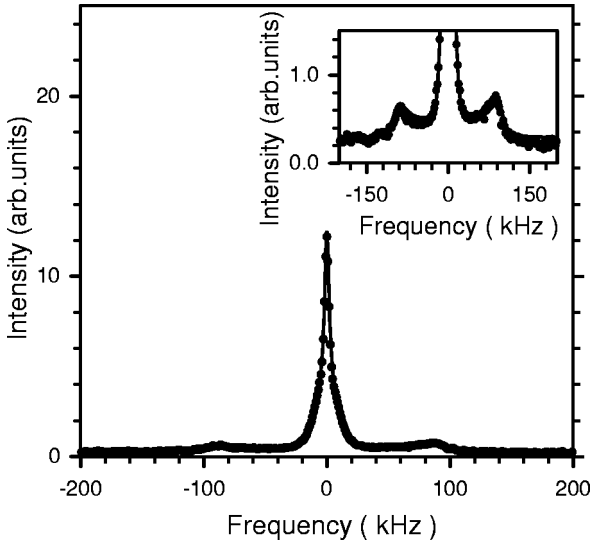

FIG. 3. The Fourier-transformed spectrum in the frequency-domain of the signal in Fig. 2. The Pake doublet from o-H_2 is shown in the inset on an expanded scale. The frequency splitting of the doublet is 176 ± 5 kHz. The solid lines are a fit to the spectrum as described in the text.

The dependence of the stimulated echo amplitude on τ_1 and τ_2 for all three components (broad, narrow, and o-H_2) in the PECVD sample is shown in Fig. 6. These data are fitted according to Eq. (2). Figure 6(a) shows the dependence on τ_2. The dependences of the echo intensities of the broad and narrow lines on τ_2 are not exponential, as reported before.[10] A phenomenological fit with two values of T_{1d} was proposed in Ref. 10. Here we adopt this approach. A more detailed discussion will be given in the following section. The intensity of the o-H_2 component can be fitted by a value of T_{1d} much larger than those of the other two components. This large value of T_{1d} is probably due to the very broad linewidth of o-H_2 that cannot be affected by fluctuations of the

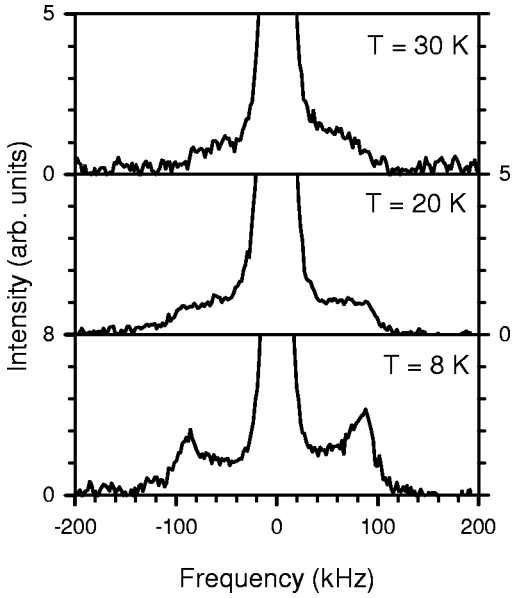

FIG. 4. Temperature dependence of the line shape from o-H_2 for the PECVD sample. The transition temperature T_c is found to be ~ 20 K.

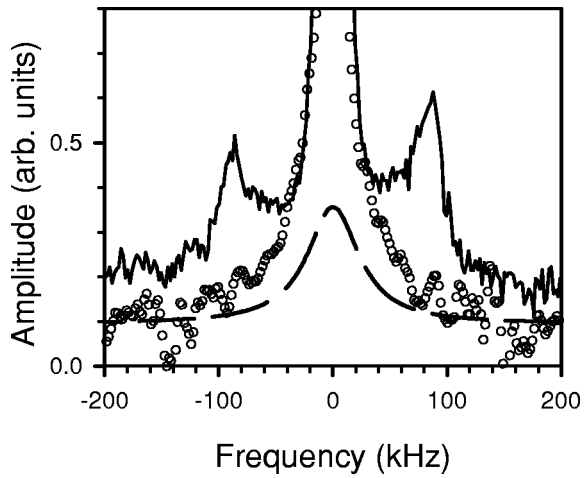

FIG. 5. Comparison of the o-H_2 line shape for the PECVD and HWCVD samples at $T=8$ K. The solid line and open circles represent the data for the PECVD and HWCVD samples, respectively. The dashed line is a fit to the narrowed Pake doublet for a HWCVD sample. The width of the fitted line is ~ 70 kHz FWHM.

dipolar fields caused by the other two components. Figure 6(b) shows the dependence on τ_1 for $\tau_2 \rightarrow 0$. All three components have a similar, larger value of T_2 (~ 400 μs). In addition, the broad line has a smaller T_2 of ~ 60 μs and the Pake doublet has a component with a smaller T_2 of ~ 70 μs.

By extrapolating the dependence to $\tau_1=\tau_2=0$, we find that the fraction of o-H_2 is $\sim 11\%$ of the total hydrogen in this sample. For HWCVD samples, the faction of o-H_2 is $\sim 1\%$ of the total hydrogen. On the other hand, the measurements of the minimum of T_1(H) at 40 K for the PECVD sample yield $T_1(\mathrm{H}) \approx 0.4$ s. From this measurement the o-H_2 concentration is inferred to be $\sim 1\%$ of the total hydrogen concentration from Eq. (1). This value is about 10% of that inferred from the stimulated echo experiments on the same sample. For the HWCVD samples, $T_1(\mathrm{H}) \sim 5$ s, which yields a fraction of o-H_2 of at most 0.1% of the total hydrogen. This value is also at most $\sim 10\%$ of that inferred from the stimulated echo experiments on the same samples. In fact, the T_1(H) in the HWCVD sample is only weakly dependent on temperature, indicating a very different spin-lattice-relaxation mechanism. These results will be discussed in the next section.

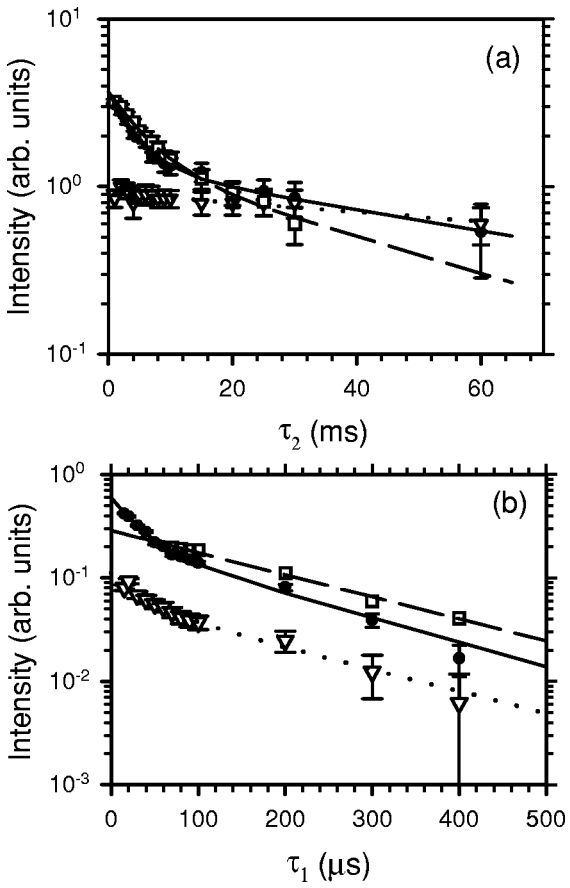

FIG. 6. The dependence of the intensities on τ_1 and τ_2 for the broad, narrow, and o-H_2 components of the PECVD sample. Solid circles, open squares, and open triangles represent the broad, narrow, and o-H_2 components, respectively. The solid line, dashed line, and dotted line are the corresponding fits to the broad, narrow, and o-H_2 components, respectively. (a) Dependence of intensities on τ_2. For the broad and narrow lines, the values of the shorter T_{1d} are ~ 4 and 6 ms, respectively. The values for the longer T_{1d} are ~ 70 and 40 ms, respectively. The T_{1d} for o-H_2 is ~ 150 ms. (b) Dependence of the intensities on τ_1 for $\tau_2=0$. The value of the longer T_2 is ~ 400 μs for all three components. The values of the shorter T_2's are ~ 60 and 70 μs for the broad line and the Pake doublet, respectively.

IV. DISCUSSION

A. Concentration of o-H_2

For both PECVD and HWCVD samples, the concentrations of o-H_2 obtained from the JB sequence are about one order of magnitude larger than those values inferred from the minima of T_1(H). In all cases, the discrepancy is much greater than the experimental error. To understand this discrepancy, $T_1(H_2)$ was measured at 40 K for the PECVD sample, using the saturating comb method described in Sec. II. Figure 7 shows the dependence on the recovery time τ for the signal from o-H_2. This figure clearly shows two very different values of $T_1(H_2)$. The larger value (~ 0.6 s) is close to that in solid hydrogen,[11] while the smaller one (~ 3 ms) agrees well with the value calculated assuming a two-phonon Raman process.[11] As suggested by these data, most of the o-H_2 molecules ($\sim 65\%$ of total o-H_2) in a-Si:H relax with a T_1 of ~ 0.6 s. Since this value of $T_1(H_2)$ is even greater than that of bonded hydrogen (~ 0.4 s), the probability for bonded hydrogen to relax through these o-H_2 is very small. Therefore these o-H_2 molecules do not participate in the relaxation of bonded hydrogen and hence cannot be detected by measurements of the minimum of T_1(H). Only those o-H_2 with smaller T_1 ($\sim 35\%$ of the total o-H_2) can relax the bonded hydrogen. The contribution of the shorter T_1 component, which can be detected by T_1(H) measurements, is $\sim 3\%$ of the total hydrogen in the PECVD sample; this number compares to $\sim 1\%$ as deduced from T_1(H) minimum experiments. These signal intensities, which are the same within experimental error, explain the discrepancy between the concentrations measured from the two different methods.

For ^{1}H NMR in solid hydrogen, the existence of a long T_1 has been known for a long time. It is known that o-H_2 in

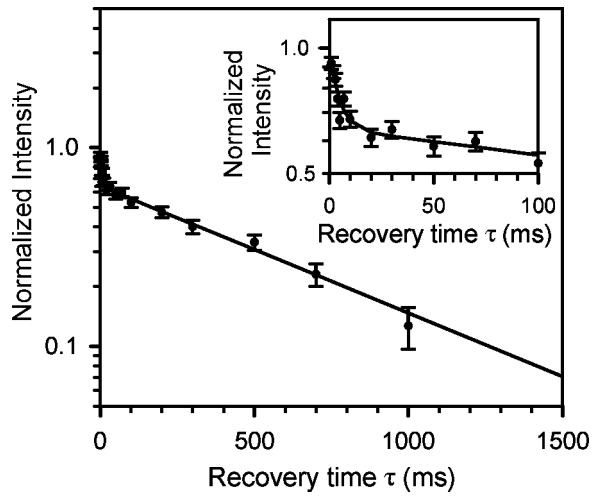

FIG. 7. Dependence of the signal intensity for o-H_2 in the PECVD sample on the recovery time τ after a saturating comb at $T=40$ K (see Sec. II for details). The signal is normalized to $I(\infty)$ and is fitted to Eq. (3). The two values of T_1 are ~ 3 ms and ~ 0.6 s. The corresponding signal fractions for the larger and smaller values of T_1 are 35% and 65%, respectively.

solid hydrogen relaxes through an electric quadrupole-quadrupole (EQQ) interaction and that $T_1(H_2)$ is independent of temperature. Nevertheless, the presence of such a long, EQQ-like $T_1(H_2)$ in a-Si:H is rather surprising, because the concentration of o-H_2 in our PECVD sample is only ~ 1 at. %, much lower than that of solid hydrogen. It has been suggested that the H_2 is trapped in microvoids, and that only the o-H_2 at the surfaces of the voids can relax through a phonon process.[11] This interpretation requires the size of the microvoids to be 20 to 30 Å, in order to obtain a volume-to-surface ratio of ~ 10. This average size is unlikely in high quality samples of a-Si:H. Drabold and Fedders studied in detail the spin-lattice relaxation of low concentration o-H_2 in a p-H_2 host.[12] These authors assumed a phonon-driven EQQ interaction between o-H_2 molecules. Their results can be summarized as follows: Two parameters, p_1 and p_2 set the scale of the interactions. They are defined as

$$p_1=\gamma/\Gamma_q \tag{4}$$

and

$$p_2=\omega_0/\Gamma_q, \tag{5}$$

where γ is the rate of direct phonon-induced transitions between the different m_J states, ω_0 is the nuclear Larmor frequency, and Γ_q is given as

$$\Gamma_q=c^{5/3}\Gamma_{\mathrm{EQQ}}, \tag{6}$$

where c is a dimensionless concentration of o-H_2 with respect to that in the solid hydrogen, Γ_{EQQ} is the coupling constant of the EQQ interaction for solid hydrogen, and $\Gamma_{\mathrm{EQQ}}\approx 0.83$ K.

When $p_1 \gg 1$, the direct phonon process dominates, and the o-H_2 can be treated as isolated molecules, which produces a temperature-dependent $T_1(H_2)$.[3] For the case $p_1 \ll 1$ and $p_2 \ll 1$, which means that the direct phonon process is insignificant and the nuclear Larmor frequency is much smaller than the EQQ interaction, the o-H_2 is in ''undominated regime,'' i.e., it experiences the effects of many neighboring molecules. In this case, a temperature-independent T_1 is given by[12]

$$T_1^{-1}=(8\pi)^{-1/2}\omega_d^2/(c^{5/3}\Gamma_{\mathrm{EQQ}}), \tag{7}$$

where ω_d characterizes the dipolar interaction between the two hydrogen atoms in an o-H_2 molecule, $\omega_d=3.62\times 10^5$ s^{-1}. Taking $\Gamma_{\mathrm{EQQ}}=0.83$ K and $T_1(H_2)\sim 0.6$ s, we find $c\sim 0.4$ with respect to the density of solid hydrogen. For a-Si:H, such a concentration is close to that where o-H_2 molecules are trapped at adjacent interstitial small voids. In this case, the average distance between the centers of two adjacent interstitial small voids is $d\sim 5$ Å.

One should note that the condition $p_2 \ll 1$ is almost always valid for typical NMR experiments, since $\Gamma_{\mathrm{EQQ}} \sim 10^{11}$ s^{-1} is much greater than any experimentally available Larmor frequency. This conclusion holds as long as c is not too small. On the other hand, c cannot be arbitrarily small for the undominated regime to survive, because at some point, the concentration will be low enough that all hydrogen molecules will be essentially isolated, i.e., $p_1 \gg 1$, and the direct phonon interaction will be more important.

A relation between temperature and concentration can be obtained to estimate a ''critical concentration'' c_0 such that, at a given temperature, when the concentration is much smaller than c_0, the direct phonon process will dominate. This concentration can be obtained by defining an average number N of neighboring o-H_2 molecules surrounding a reference o-H_2, for which the EQQ interaction is greater than the direct phonon interaction. N is given as[12]

$$N\approx 4\pi(\sqrt{2}/3)(\Gamma_q/\gamma)^{3/5}, \tag{8}$$

where Γ_q is given in Eq. (6) above. The concentration c_0 can be estimated by setting N to be unity. Near c_0, o-H_2 is in the ''dominated regime,''[12] i.e., it feels a strong EQQ from only one neighboring o-H_2 molecule. In this regime, T_1 assumes a more complicated dependence on temperature, concentration, and magnetic field. Only when $c \ll c_0$ can the relaxation be characterized as a phonon-dominated process.

The temperature dependence of γ is given by $\gamma=AT^7$ for $T \ll \Theta_D$, and $\gamma=BT^2$ for $T \gg \Theta_D$,[13] where Θ_D is the Debye temperature. Conradi *et al.* found that $\Theta_D\approx 40$ K for o-H_2 in both a rare gas and a p-H_2 host.[14] We find that a similar value fits T_1(H) in a-Si:H. These authors also found that fitting γ at 40 K using $\gamma=AT^7$ gives satisfactory results.[14] Their results yield a value of γ at 40 K of about 10^9 s^{-1}. For $T=40$ K, where the T_1(H) minimum occurs in a-Si:H, we estimate $c_0\approx 0.01$, using the values described above for o-H_2 in rare-gas host. This value means that the phonon-induced relaxation of o-H_2 can only happen at concentrations much lower than 1 at.%. Experimentally, for our PECVD sample, we find the concentration of o-H_2 that relaxes through a phonon-induced process is only ~ 1% of the total hydrogen, or about one-tenth of c_0 as given above. This estimate assumes a total hydrogen concentration of about 10 at. %. Similar results are obtained for the HWCVD samples, where the concentration of o-H_2 that relaxes through a phonon process is at most 0.003 at. %, for ~ 3 at. % hydrogen incorporation. In addition, we do not

observe strong evidence for values of T_1 of o-H_2 that correspond to the cases between these two extremes. Therefore there is no broad distribution of the concentrations of H_2. We are lead to the conclusion that in a-Si:H, there are two types of sites for H_2: (1) the essentially isolated H_2 that can relax the bonded hydrogen, and (2) the clustered H_2 that relaxes through the EQQ interaction and does not contribute to the relaxation of bonded hydrogen, the latter site probably consists of o-H_2 trapped in adjacent, interstitial voids.

B. Spin-lattice-relaxation mechanism in HWCVD samples

In contrast to the typical PECVD samples, which exhibit a strong temperature-dependent T_1(H), the HWCVD samples have a T_1(H) that is weakly dependent on the temperature and much longer at the temperature where the minimum in T_1 is expected. For the HWCVD samples, T_1(H) is approximately equal to 5 s at $T=40$ K, where the minimum is expected. This value is about one order of magnitude larger than that of the typical PECVD samples. One possible mechanism for such a behavior is the relaxation through rapidly relaxing paramagnetic centers, such as silicon dangling bonds. However, an estimated density of dangling bonds of $\sim 10^{18}$ cm^{-3} is needed to produce such a value, assuming a homogeneous spatial distribution of the dangling bonds. This density is much too large for these materials. Another possibility is that the bonded hydrogen relaxes through those clustered o-H_2, molecules that relax through a temperature-independent EQQ interaction. Nevertheless, for EQQ-induced relaxation [$T_1(H_2)\sim 0.6$ s], the concentration of o-H_2 must be $\sim$10% of the total hydrogen to produce a T_1(H) of ~ 5 s. This concentration is about one order of magnitude higher than observed (see Sec. IV A). The third possibility is spin-diffusion-limited relaxation through those o-H_2 molecules that have a phonon-induced T_1 of ~ 3 ms. In this case, $T_{1(SD)}$ is[2]

$$T_{1(SD)}^{-1}=4\pi D\frac{3}{4}n(H_2)b, \tag{9}$$

where b is the average distance between o-H_2 and the nearest bonded H, and $n(H_2)$ is the concentration of o-H_2 that contributes to T_1(H). D is the spin-diffusion constant, and one calculation gives D as[15]

$$D=\frac{d^2}{30\langle T_2\rangle}, \tag{10}$$

where d is the average distance between bonded hydrogen atoms and $\langle T_2\rangle$ is the averaged T_2 for the entire NMR line. However, this formula, which applies to a homogeneous system, is not particularly appropriate for the HWCVD samples. In these samples, a large portion of the hydrogen is heavily clustered with a $\langle T_2\rangle$ much smaller than that of the PECVD sample, even though the hydrogen concentration is much lower than that of PECVD samples. A more refined model,[16] due to Fedders, is also inappropriate because of the inhomogeneous distribution of hydrogen atoms.

We argue here that the diffusion time in HWCVD samples is mainly determined by the diffusion among the dilute hydrogen atoms, and therefore the average T_2 should be taken as the average of the narrow line that arises from the dilute hydrogen. Although the nuclear spins can quickly thermalize within the cluster, as reflected by the much shorter T_2 of the broad line, it will take a much longer time for the spin to diffuse beyond the cluster. This argument is similar to that concerning the region near an o-H_2 molecule in the case of diffusion-limited relaxation,[16] where the details of the diffusion near o-H_2 are not important as long as the concentration of o-H_2 is small. A more general discussion of spin diffusion can be found in Ref. 17.

For our HWCVD samples, the hydrogen concentration is ~ 3 at.%, and about 70% of the hydrogen is in clustered sites. If we treat each of these clusters as a single site that quickly thermalizes, then the effective concentration is ~ 2 at. %, which yields $b\approx d\approx 6$ Å. A hole-burning experiment gives an intrinsic linewidth δ of ~ 0.5 kHz for the narrow line,[18] which sets the scale of the dipolar interaction and therefore the transfer rate of magnetization between two adjacent spins. A rough estimate of the $\langle T_2\rangle$ of the dilute hydrogen is

$$\langle T_2\rangle=(\pi\delta)^{-1}\approx 700\ \ \mu s. \tag{11}$$

By taking $n(H_2)$ to be at most 0.1% of the total hydrogen, $T_{1(SD)}$ is estimated to be at least 5 s. On the other hand, for the same $n(H_2)$, at $T=40$ K, the relaxation time through o-H_2, which is the first term in Eq. (1), is ~ 1.5 s. This value is smaller than $T_{1(SD)}$ estimated above. Such a qualitative estimate suggests that the relaxation process in HWCVD samples is probably spin-diffusion-limited, resulting in a weak temperature dependence.

C. Hydrogen distributions in a-Si:H

Using results from deuterium NMR (DMR) of a-Si:H,D and a-Si:D, Norberg *et al.* have suggested that the entire narrow line is due to molecular hydrogen, instead of dilute, bonded hydrogen.[19] To investigate the relationship between the molecular hydrogen and the narrow line, we compare the line shapes at 8 K and at room temperature for the PECVD sample, as shown in Fig. 8. At 8 K the signal fractions for the broad, narrow, and Pake doublet lines from o-H_2 are 60%, 30%, and 10%, respectively. At room temperature, the fractions are 60% and 40% for broad and narrow lines, respectively. The signal from o-H_2 has narrowed to a line with width similar to that of the narrow line. Therefore, only $\sim$25% of the narrow line is due to molecular hydrogen.

This argument is also supported by other experimental evidence. First, the narrow line persists even at $T=1.4$ K, and its fraction is almost independent of temperature below $T_c\sim 20$ K.[5] This result means that any additional o-H_2 molecules that may contribute to the narrow line must reside in the sites with negligible EFG from the silicon matrix, since they do not freeze out even at 1.4 K. This situation is unlikely for an amorphous material because the EFG is highly sensitive to distortions of the lattice.

Second, hole-burning experiments show that the intrinsic linewidth of the narrow line is ~ 0.5 kHz.[18] This value indicates a strong dipolar broadening. Since the gyromagnetic ratio of o-H_2 is much smaller, significant clustering is needed for o-H_2 to broaden the line to ~ 4 kHz. We estimated that the local concentration of o-H_2 needs to be ~ 20 to 30 at. % to broaden the line to ~ 4 kHz. Taking into

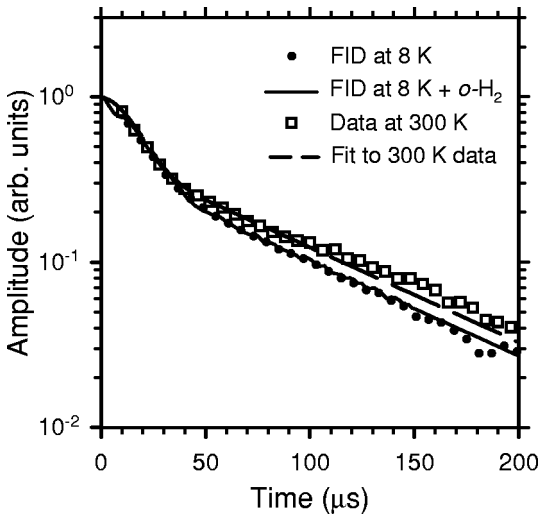

FIG. 8. Comparison of the time-domain free-induction decays (FID) at $T=300$ K and $T=8$ K for the PECVD sample. The solid line is the observed FID at 8 K, superimposed with a 10% contribution from the o-H_2 signal. The signal fractions of the broad and narrow central lines are 60% and 30% at 8 K and 60% and 40% at 300 K, respectively. The deviation from exponential decay in the 300 K data at long times is probably an artifact due to the equipment.

account that the lattice constant for silicon is only ~ 2.35 Å, compared to 3.8 Å for solid hydrogen, this width yields an o-H_2 density close to that in solid hydrogen. As mentioned in Sec. IV A, such a clustering will result in a strong EQQ interaction between o-H_2 molecules, which is comparable to that in solid hydrogen. If the entire narrow line is due to molecular hydrogen, then, since one would expect T_c to be similar to that for solid hydrogen, the entire narrow line should freeze into a Pake doublet below about 1.4 K. This behavior is not observed.[5] In addition, if the entire narrow line arises from highly clustered hydrogen molecules, one would expect a temperature-independent, EQQ-induced T_1 for the narrow line; however, almost all experimental evidence shows that the T_1 of the narrow line has the same strong temperature dependence as for the broad line, which arises from the clustered, bonded hydrogen.

The third and most important evidence is from ortho-para conversion experiments,[4] where the isolated o-H_2 concentration is reduced by more than factor of 5 by annealing at 4.2 K for several months. Since the ortho-para conversion process is a bimolecular process and strongly depends on the density of o-H_2,[20] the clustered o-H_2 converts much faster than the isolated o-H_2. Therefore, if the entire narrow line is due to o-H_2, the total concentration of o-H_2 will be reduced much more than a factor of 5, then the intensity of the narrow line will drop to the order of $\sim 5-10\,\%$ of its original intensity. Such a reduction is not observed in the experiments.

D. Temperature dependence of the o-H_2 line shape and the effect of the silicon lattice

As mentioned in Sec. I, the EFG from the silicon matrix contributes most of the anisotropic crystal field, and hence determines the transition temperature T_c. For an ideal symmetric crystal, such as silicon, the symmetry of lattice causes a cancellation of the EFG from neighboring lattice sites and the net EFG at the center of an interstitial site vanishes. However, the distortion of bond angles and bond lengths in a-Si:H can result in a nonvanishing EFG at the center of an ''interstitial'' site. Therefore, T_c is very sensitive to the distortions of the lattice. A more ordered lattice will produce a smaller EFG and reduce T_c, causing motional narrowing of the Pake doublet even at low temperatures. As shown in Fig. 5, the motional narrowing of the Pake doublet for the HWCVD samples suggests that T_c is much lower for these samples than it is for PECVD samples. Such a low T_c is indicative of a much more ordered silicon matrix for HWCVD samples. Since the EFG strongly depends on the distortion of the lattice, and $T_c \sim 1.6$ K in solid hydrogen, we believe that T_c for these materials is very close to that in solid hydrogen; i.e., the local bonding configuration of the silicon matrix for the HWCVD samples is very close to that of crystalline silicon. In fact, such a crystallinelike behavior has also been observed by measuring the internal friction of similar samples.[21] For typical amorphous materials, it is well known that the disordered atomic structure induces low-energy excitations, which produce a significantly higher internal friction than in crystalline materials at low temperature. Recent results from internal friction measurements on similar HWCVD samples have shown that the internal friction of these materials is within the background of the crystalline silicon substrates.[21] These measurements also suggest that the HWCVD samples have a very ordered bonding structure.

The details of the local environments of these hydrogen molecules are still not clear. X-ray diffraction experiments on similar HWCVD samples showed that the size of the voids is less than 10 Å, and the volume fraction of the voids is less than 0.1%.[22] It is unlikely that there exist large voids filled with hydrogen molecules in these films. Also, the x-ray diffraction and Raman scattering experiments show that these HWCVD samples are still amorphous; therefore, the ordered region must be local, probably only within a distance of several interatomic spacings. Small, highly ordered regions have been found in so-called protocrystalline a-Si:H made by the PECVD technique with high hydrogen dilution.[23–25] In these materials, small crystallinelike regions are observed, although x-ray diffraction shows that these films are still amorphous. For a-Si:H films made without hydrogen dilution, similar small, crystallinelike regions are also found by variable coherence microscopy.[26] These so-called paracrystallites are topologically crystalline but amorphous as observed in x-ray diffraction.[26] The existence of these paracrystallites has been reported recently in studies of a-Si:H thin films made by various techniques, including PECVD, HWCVD and sputtering.[27] The sizes of these paracrystallites are about 1 to 3 nm, which are too small to be detected by x-ray diffraction or Raman scattering, yet large enough to incorporate several hydrogen molecules. One possibility of the local environments of the H_2 molecules is that these H_2 molecules are trapped in the small crystalline region or at the crystalline-amorphous boundary. This suggestion is consistent with the fact that most of the hydrogen molecules are clustered in HWCVD samples. Further experiments are needed to clarify this issue.

E. Dipolar spin-lattice relaxation of the bonded hydrogen

Previous work on the dipolar spin-lattice relaxation of bonded hydrogen has shown the dependence of T_{1d} on the defect concentration and doping of the materials.[28] Since the signal-to-noise ratio limited the measurement to the short-time region of the T_{1d}, these results showed exponential behavior. The dipolar spin-lattice relaxation was ascribed to the local motion of these hydrogen atoms. However, there are some difficulties in relating the relaxation to local motion of the hydrogen. First, it is found that for temperatures below 200 K, both the long T_{1d} and the short T_{1d} are almost independent of the temperature.[10] At 8 K, the value of the short T_{1d} is almost the same as that at 300 K, while a thermally activated process would result in a much longer T_{1d}. Second, there is no motional narrowing of the bonded hydrogen up to room temperature. Therefore, τ_c, the time between two jumps of a spin, cannot be estimated by $\tau_c \approx T_2$.[28] Moreover, T_{1d} strongly depends on the defect density or doping level. Since the defect density ($\sim 10^{15}$ cm^{-3}) is much lower than the hydrogen concentration ($\sim 10^{21}$ cm^{-3}), it is difficult to understand how such a small concentration of electrons can influence the motion of so many hydrogen atoms.

On the other hand, as shown in Fig. 4, the dipolar spin-lattice relaxation during τ_2 is not exponential. Similar behavior is also found in Ref. 10. Although a phenomenological fit with two values of T_{1d} gives satisfactory agreement with the experimental data, the underlying physical mechanism is not clear. In particular, it is not clear why both the narrow line and the broad line exhibit similar values of T_{1d}, despite their very different environments. We found that such a nonexponential decay can be fitted by assuming

$$I(\tau_2) \sim \exp\{-(\tau_2/\tau)^{1/2}\}, \tag{12}$$

as shown in Fig. 9. The values of τ are 7.3 ms and 8.6 ms for the Lorentzian and Gaussian components, respectively. These values are identical within experimental error. This behavior is well known for the case of spin-lattice relaxation by paramagnetic centers without spin diffusion,[29,30] and the nonexponential behavior is due to inhomogeneous relaxation.[31] In the following paragraphs we outline an alternative interpretation to local motion, one that incorporates the dependence of T_{1d} on the defects and doping in a more natural manner. Although admittedly crude, such an approach sheds some light on the further understanding of the phenomenon.

A typical PECVD sample contains density of paramagnetic defects of $\sim 10^{15}$ cm^{-3}. These defects can be detected by electron-spin-resonance (ESR). The average distance between two electrons is $d_e \sim 10^{-5}$ cm. The total Hamiltonian including both the nuclei and electrons is

$$\mathcal{H} = \mathcal{H}_{ZI} + \mathcal{H}_{ZS} + \mathcal{H}_{DII} + \mathcal{H}_{DIS} + \mathcal{H}_{DSS}, \tag{13}$$

where $\mathcal{H}_{ZI}$ and $\mathcal{H}_{ZS}$ are the Zeeman Hamiltonians for the nuclei and electrons, respectively. The last three terms represent the secular part of the total dipolar Hamiltonian of the system. $\mathcal{H}_{DII}$ and $\mathcal{H}_{DSS}$ are nuclear-nuclear and electron-electron dipolar energies, respectively, and $\mathcal{H}_{DIS}$ is the dipolar interaction between the nuclei and the electrons. For systems with two types of spins, the total dipolar energy, including interactions between both like and unlike spins, is

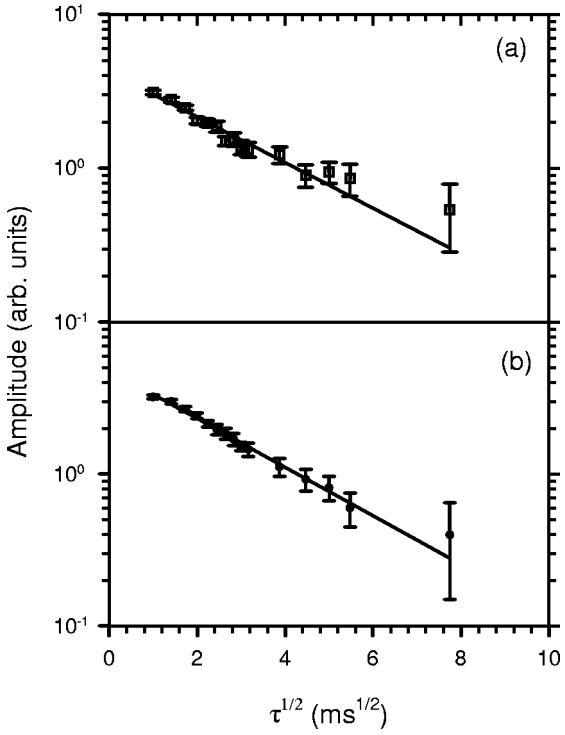

FIG. 9. Fit to the τ_2 dependence of the echo intensity according to Eq. (12). (a) fit to the Gaussian component, and (b) Fit to the Lorentzian component. Open squares and solid circles represent Gaussian and Lorentzian components, respectively. Solid lines are the corresponding fits. The values of τ are 8.6 ms and 7.3 ms for the Gaussian and Lorentzian components, respectively.

a constant of motion.[32] Therefore, the electrons and the hydrogen atoms form a single dipolar reservoir that, at internal equilibrium, has a common dipolar spin temperature. (A detailed discussion of the thermodynamics of the spin system is given by Jeener *et al.*[33]) Right after the second pulse of the JB sequence, the dipolar energy of the hydrogen atoms increases, but the entire dipolar system, including both electrons and the hydrogen, is far from internal equilibrium. During the time following the second pulse, the dipolar energy is redistributed between the hydrogen atoms and the electrons to establish a common dipolar spin temperature. Because the electronic dipolar system is initially at the lattice temperature, such a process effectively cools the nuclear dipolar system. During this cooling the dipolar energy of the nuclear system decreases and the dipolar energy of the electronic system increases. Such behavior has been reported for LiF where after preparing the dipolar order in the ^{19}F system, a simultaneous decrease of ^{19}F dipolar energy and increase of ^{7}Li dipolar energy is observed.[34] If the spin diffusion between nuclei is rapid compared to the rate of energy exchange between the nuclei and the electrons, the time needed to reach an internal equilibrium is determined by the relative heat capacities of the nuclear and the electronic dipolar systems. In this case, a characteristic time τ_c is of the form similar to Eq. (1). However, using d_e estimated above, a spin-diffusion bottleneck is estimated to occur at $\sim 10^5$ s, much larger than the experimentally observed value. Therefore the relaxation will be determined by the direct rate of energy exchange between each nuclei and the electrons, a process in which spin diffusion is not important.

The above process can occur under two scenarios. If the electrons have good thermal contact with the lattice, then the approach to internal equilibrium in the dipolar reservoir will be controlled effectively by the dipolar spin-lattice relaxation of the entire system. If not, then one would expect first the establishment of the internal equilibrium discussed above, and then the entire dipolar reservoir will relax toward the lattice temperature with a much longer time scale. In either case, the initial decrease of the dipolar signal of the nuclei will depend on the concentration of the paramagnetic electrons, which is related to silicon dangling bond density and the doping level. For *a*-Si:H, the first situation is most likely because the spin-lattice-relaxation time of the electrons is much shorter than that of hydrogen ($T_1 \sim 10$ ms at 8 K).[35] Any calculation of the dependence on the electron density is complicated by the fact that the dipolar interaction between nuclei and electrons varies over a wide range. However, Stöckmann and Heitjans pointed out that, for the case where spin-diffusion is not important, Eq. (12) generally holds if the coupling constant $a(r)$ takes the form[31]

$$a(r) = a_0 \left(\frac{r_0}{r} \right)^6 , \tag{14}$$

where r_0 is the distance between the defect and its nearest neighbor and a_0 the corresponding coupling constant. The distance r is between the defect and the reference nucleus. In this case τ, defined in Eq. (12), will be proportional to N_p^{-2}, where N_p is the density of paramagnetic defects. Using the data reported in Ref. 28, the ratio of defect density before and after light-soaking is $N_p^{(i)}/N_p^{(f)} \approx \frac{1}{2}$. The corresponding ratio of T_{1d} is $T_{1d}^{(i)}/T_{1d}^{(f)} \approx 3$, which qualitatively agrees with the argument presented above.

Several experiments can be performed to test this interpretation. One is to illuminate the sample at low temperature to create large amount of the paramagnetic electrons and holes trapped in band-tail states. If the above argument is correct, this dramatic increase in N_p should result in a significant reduction of T_{1d} as expected. Also one may disturb the electronic system by applying a microwave field at the resonance frequency of the electrons after the second pulse, and monitor the effect on the nuclear dipolar order. The third experiment is to measure $T_{1\rho}$, the spin-lattice-relaxation time in the rotating frame, which should depend on the field as ω^{-2} and on the time as shown in Eq. (12). On the other hand, motion-induced relaxation should be independent of the field. The fourth experiment is an electron-nuclear double-resonance (ENDOR) experiment. If one can measure the dipolar signal of the electrons, then by preparing the nuclear system with dipolar order and monitoring the electronic signal, the change of the electronic dipolar energy should be observable.

V. SUMMARY

In summary, the concentration of molecular hydrogen in *a*-Si:H was found to be about 10% of the total hydrogen incorporated in the PECVD sample and ~1% in the HWCVD samples. There are two types of sites for these hydrogen molecules, one in which the hydrogen molecules are isolated and contribute to spin-lattice relaxation of bonded hydrogen, and another in which they are clustered and do not participate the spin-lattice relaxation of the bonded hydrogen. Comparison of the line shapes at 8 K between the PECVD and HWCVD samples suggests that the HWCVD samples have a more ordered silicon matrix. Also, only ~25% of the narrow line at room temperature is due to molecular hydrogen, a fact that confirms the existence of isolated, bonded hydrogen atoms in these materials. Finally the nonexponential dipolar relaxation probably reflects an approach to the internal equilibrium of the entire dipolar system including both nuclei and electrons. Therefore this relaxation depends quite naturally on the defect density and the doping level.

ACKNOWLEDGMENTS

We thank John Viner for his great help on the experimental procedures. We also acknowledge helpful discussions with P. A. Fedders and David A. Ailion. The work done at the University of Utah is supported in part by NSF under Grant No. DMR-9704946 and by NREL under Subcontract No. XAK-8-17619-13.

[1] Jeffrey A. Reimer, Robert W. Vaughan, and John Knights, Phys. Rev. Lett. **44**, 193 (1980); Phys. Rev. B **24**, 3360 (1981).
[2] M. S. Conradi and R. E. Norberg, Phys. Rev. B **24**, 2285 (1981).
[3] P. A. Fedders, Phys. Rev. B **20**, 2588 (1979).
[4] W. E. Carlos and P. C. Taylor, Phys. Rev. B **25**, 1435 (1982); **26**, 3605 (1982).
[5] J. B. Boyce and M. Stutzmann, Phys. Rev. Lett. **54**, 562 (1985).
[6] C. G. Van de Walle, J. Non-Cryst. Solids **227-230**, 111 (1998).
[7] I. F. Silvera, Rev. Mod. Phys. **52**, 393 (1980).
[8] F. Reif and E. M. Purcell, Phys. Rev. **91**, 631 (1953).
[9] J. Jeener and P. Broekaert, Phys. Rev. **157**, 232 (1967).
[10] P. H. Chan, Ph.D. thesis, Washington University, 1993.
[11] P. A. Fedders, R. Fisch, and R. E. Norberg, Phys. Rev. B **31**, 6887 (1985).
[12] D. A. Drabold and P. A. Fedders, Phys. Rev. B **39**, 6325 (1989).
[13] J. van Kranendonk, Physica (Utrecht) **20**, 781 (1954).
[14] Mark S. Conradi, K. Luszczynski, and R. E. Norberg, Phys. Rev. B **20**, 2594 (1979).
[15] G. R. Khutsishvili, Usp. Fiz. Nauk **87**, 211 (1965) [Sov. Phys. Usp. **8**, 743 (1966)].
[16] P. A. Fedders, Phys. Rev. B **32**, 2739 (1985).
[17] A. Abragam, *The Principle of Nuclear Magnetism* (Oxford University Press, London, 1961), p. 378.
[18] J. Todd Stephen, Daxing Han, A. Harv Mahan, and Yue Wu, in *Amorphous Silicon Technology-1996*, edited by Micheal Hack *et al.*, MRS Symposia Proceedings No. 420 (Material Research Society, Pittsburgh, 1996), p. 485.
[19] R. E. Norberg, D. J. Leopold, and P. A. Fedders, J. Non-Cryst. Solids **227-230**, 124 (1998).
[20] A. John Berlinsky and Walter N. Hardy, Phys. Rev. B **8**, 5013 (1973).
[21] Xiao Liu, B. E. White, Jr., and R. O. Pohl, Phys. Rev. Lett. **78**, 4418 (1997).

[22] S. Acco, S. L. Williamson, S. Roorda, W. G. J. H. M. van Sark, A. Polman, and W. F. van der Weg, J. Non-Cryst. Solids **227-230**, 128 (1998).
[23] J. Koh, Y. Lee, H. Fujiwara, C. R. Wronski, and R. W. Collins, Appl. Phys. Lett. **73**, 1526 (1998).
[24] D. V. Tsu, B. S. Chao, S. R. Ovshinsky, S. Guha, and J. Yang, Appl. Phys. Lett. **71**, 1317 (1997).
[25] A. H. Mahan, J. Yang, S. Guha, and D. L. Williamson, Phys. Rev. B **61**, 1677 (2000).
[26] M. M. J. Treacy, J. M. Gibson, and P. J. Keblinski, J. Non-Cryst. Solids **231**, 99 (1998).
[27] P. M. Voyles, H-C. Jin, J. R. Abelson, J. M. Gibson, and M. M. J. Treacy, in *Amporphous and Heterogeneous Silicon Thin Filme-2000*, edited by R. W. Collins *et al.*, MRS Symposia Proceedings No. 609 (Materials Research Society, Pittsburgh, 2000), p. A.2.4.1.
[28] P. Hari, P. C. Taylor, and R. A. Street, in *Amorphous Silicon Technology-1994*, edited by Eric, A. Schiff *et al.*, MRS Symposia Proceeding No. 336 (Materials Research Society, Pittsburgh, 1994), p. 293; in *Amorphous Silicon Technology-1995*, edited by Michael Hack *et al.*, MRS Symposia Proceedings No. 377 (Materials Research Society, Pittsburgh, 1995), p. 185 and references therein.
[29] D. Tse and S. R. Hartmann, Phys. Rev. Lett. **21**, 511 (1968).
[30] I. J. Lowe and D. Tse, Phys. Rev. **166**, 279 (1968).
[31] H. -J. Stöckmann and P. Heitjans, J. Non-Cryst. Solids **66**, 501 (1984).
[32] Harold T. Stokes and David A. Ailion, Phys. Rev. B **16**, 4746 (1977).
[33] J. Jeener, H. Eisendrath, and R. Van Steenwinkel, Phys. Rev. **133**, A478 (1964).
[34] P. Broekaert and J. Jeener, Phys. Rev. B **15**, 4168 (1977).
[35] M. Stutzmann and D. K. Biegelsen, Phys. Rev. B **28**, 6256 (1983); **34**, 3093 (1986).